ARTICLE

Silica–surface reorganization during organotin grafting evidenced by ^{119}Sn DNP SENS: a tandem reaction of gem-silanols and strained siloxane bridges

Matthew P. Conley,[a] Aaron J. Rossini,[b] Aleix Comas Vives,[a] Maxence Valla,[a] Gilles Casano,[c] Olivier Ouari,[c] Paul Tordo,[c] Anne Lesage,[b] Lyndon Emsley,[b,]* Christophe Copéret[a,]*

Grafting reactive inorganic species on dehydroxylated amorphous silica is a strategy to develop "single-site" heterogeneous catalysts. In general, only the reactivity of isolated silanols is invoked for silica dehydroxylated at 700 °C ([$SiO_{2\text{-}700}$]), though *ca.* 10 % of the surface silanols are in fact geminal Q_2-silanols. Here we report the reaction of allyltributylstannane with [$SiO_{2\text{-}700}$] and find that the geminal Q_2-silanols react to form products that would formally arise from vicinal Q_3-silanols that are not present on [$SiO_{2\text{-}700}$], indicating that a surface rearrangement occurs. The reorganization of the silica surface is unique to silica dehydroxylated at 700 °C or above. The findings were identified using Dynamic Nuclear Polarization Surface Enhanced NMR Spectroscopy (DNP SENS) combined with DFT calculations.

Introduction

Amorphous silica, a common support for heterogeneous catalysts, is composed of bulk tetrahedral SiO_4 units as well as silanol ($\equiv$Si-OH) and siloxane bridge ($\equiv$Si-O-Si$\equiv$) surface functionalities. Control of the type and quantity of silanols present on the silica surface is critical, particularly for the generation of 'single-site' heterogeneous catalysts.[1-3] Three different types of silanols are on the silica surface: vicinal Q_3-, geminal Q_2-, and isolated Q_3-silanols (Figure 1). Applying high temperatures under vacuum leads to a dehydroxylation process, which slowly removes vicinal (hydrogen-bonded) silanols by condensation and elimination of water. After 4 hours of treatment at 700 °C silica reached a low silanol density (ca. 0.8 SiOH nm^{-2}) without significant loss of surface area; the surface contains mainly isolated non-hydrogen bonded Q_3-isolated silanols ($\equiv$SiOH). They have thus been widely used to prepare surface complexes $\equiv$ SiO-ML$_n$ by reaction with an appropriate molecular complex X-ML$_n$ containing a labile X anionic ligand to generate well-defined surface species in much the same way a molecular silanol would react in solution. With this approach, a range of mono-siloxy surface species have been prepared and used as so-called single-site supported catalysts.[3-5]
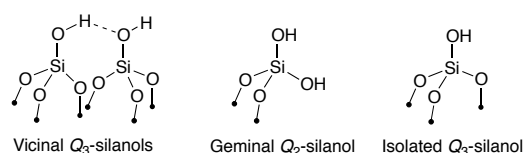

Figure 1. Silanols present on the silica surface.

The infrared spectrum of silica dehydroxylated at 700 °C [$SiO_{2\text{-}700}$] contains a sharp symmetric ν_{OH} band at 3745 cm^{-1} associated with mainly isolated silanols. However, previous works have shown that [$SiO_{2\text{-}700}$] also contains residual geminal Q_2-disilanols (*ca.* 0.13 $\equiv$Si(OH)$_2$ nm^{-2}),[6] which have a similar IR signature (within 2 cm^{-1}) since the two silanol moieties, while adjacent, are not H-bonded.[7,8] In fact, the ^{29}Si Cross Polarization Magic Angle Spinning (CPMAS) NMR spectrum of [$SiO_{2\text{-}700}$] under inert anhydrous conditions contains resonances for both Q_3-isolated silanols and Q_2-geminal di-silanols (see Supporting Information Figure S1).[9] The Q_2-species are typically not considered in the grafting process of organometallic complexes on [$SiO_{2\text{-}700}$].

Here we explore the reactivity of the Q_2-species. In view of the reactivity of organotin reagents with surface silanols,[10-12] and the impact these functionalities can have on the adsorption of gases in tin functionalized materials,[13] we investigate the reaction between silicas partially dehydroxylated between 300 and 1000 °C with allyltributylstannane, Bu$_3$Sn(allyl). This particular organostannane was chosen because it contained two types of Sn-C bonds: the Sn-allyl is more reactive towards surface silanols[14] and will liberate propene upon grafting, while the cleavage of the Sn-butyl to form *bis*-grafted tin species and butane is much slower, and typically happens only at higher temperatures (> 100 °C).[10] The formation of *bis*-grafted tin species would occur only as a secondary reaction, allowing us to differentiate the surface silanol sites. The large chemical shift range of ^{119}Sn and its sensitivity to chemical environment make ^{119}Sn solid-state NMR an ideal tool to probe the structure of organotin surface species. Dynamic Nuclear Polarization Surface Enhanced NMR (DNP SENS)[15-17] is utilized here to

overcome the low sensitivity of solid-state NMR and enable fast characterization of the different materials. In combination with [119]Sn DNP SENS,[18] first principles calculations show that the Q_2-geminal silanols present in [SiO$_{2\text{-}700}$], while reactive, do not lead to the formation of tin species directly bonded to each Q_2-silanol (*i.e.* [=Si(O)$_2$SnBu$_2$]/[=Si(OH)(OSnBu$_3$)]), but rather to [(≡SiO)$_2$SnBu$_2$], a compound that corresponds formally to the product of the grafting of allyltributylstannane with two adjacent Q_3-vicinal silanols, but which arises from the grafting on a Q_2-silanol followed by a surface rearrangement involving the opening of adjacent strained siloxane bridges

Results

Grafting Bu$_3$Sn(allyl) on Dehydroxylated Silica

Scheme 1 shows the expected reaction products between Bu$_3$Sn(allyl) and the different types of surface silanols. Isolated silanols are expected to form [(≡SiOSnBu$_3$)] and liberate propene. Q_2-geminal silanols can react with allyltributylstannane to form the monografted [(=Si(OH)(OSnBu$_3$)] with one equivalent of propene. Further reaction can in principle form the *bis*-grafted [=Si(O)$_2$SnBu$_2$] from the direct reaction of a Sn-Bu group with the remaining silanol. The formation of *bis*-grafted species would be evidenced by the presence of butane in the volatile fraction. Finally, vicinal Q_3-silanols could react to form either a monografted Sn species with a nearby silanol or *bis*-grafted[(≡SiO)$_2$SnBu$_2$] species. Note that vicinal Q_3-silanols could also yield two adjacent monografted Sn species.
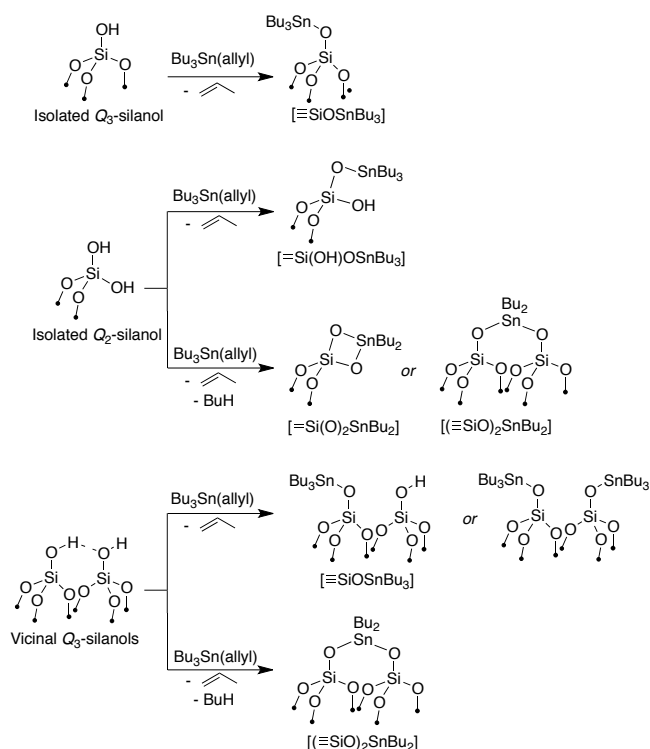
Scheme 1. Expected products from grafting allyltributylstannane on the different types of surface silanols.

Contacting [SiO$_{2\text{-}700}$] and allyltributylstannane in toluene at 110 °C for 3 days results in consumption of most of the surface silanols, evidenced by the lack of a strong ν_{OH} and the presence of expected ν_{CH} vibrational bands in the infrared spectrum. Quantitative mass balance analysis showed that 0.95 equivalents of propylene and 0.07 equivalent of butane were evolved per surface silanol during the grafting. From these results we infer the formation of the *mono*-grafted [(≡SiO)SnBu$_3$] and a *bis*-grafted tin species (Scheme 1). We should note that the presence of butane in the volatiles indicates that *ca.* 8 % of surface silanols contain nearby OH groups, which likely originate from Q_2-geminal silanols (10 %) in view of the absence of Q_3 vicinal silanols. The ^{13}C CPMAS NMR spectrum contains resonances for only the butyltin carbons. Note that no signal associated with alkylsilicon surface species (expected around 0 ppm) was observed (Figure S5). The ^{29}Si CPMAS NMR spectrum contains a broad signal associated with Q_4-bulk silica sites and *Si*-O-Sn silicon species,[19] indicating that alkyl transfer to silica did not take place under these conditions, and that all Q_2- and Q_3-silanol sites have been consumed (Figure S1). This observation is notable since transfer of alkyl or hydride ligands to the silica surface is a commonly encountered process when reactive metal centres are near strained siloxane bridges that are present on silica partially dehydroxylated at high temperature (> 700 °C).[20-22]

Silicas dehydroxylated at either 800 or 1000 °C ([SiO$_{2\text{-}800}$] and [SiO$_{2\text{-}1000}$]), which also contain isolated Q_3 and Q_2 silanols (Figure S2 and S3), also react with allyltributyltin under these conditions. Analyses of the volatiles from these reactions establish that butane is present and that also in these cases *ca.* 6 % of the surface silanols contain nearby OH groups. Surprisingly, volatile analysis of the reaction of allyltributyltin with [SiO$_{2\text{-}500}$] or [SiO$_{2\text{-}300}$], which contain high surface silanol density (up to 2.8 SiOH nm^{-2} on [SiO$_{2\text{-}300}$]) and large amounts of vicinal silanols (1.4 SiOH nm^{-2} for [SiO$_{2\text{-}300}$]), only contain traces of butane (0.05 % and 0.1 %, respectively). The infrared spectrum of these materials contains a broad ν_{OH}, indicating that some silanols present on [SiO$_{2\text{-}500}$] and [SiO$_{2\text{-}300}$] do not react with allyltributyltin.

[119]Sn DNP SENS Studies Direct evidence of the structures of the *mono*-grafted [≡SiOSnBu$_3$] and *bis*-grafted surface species was obtained using solid-state NMR spectroscopy. Though the NMR properties of [119]Sn (8.6 % abundance, $\gamma/2\pi$ = 15.86 MHZ T^{-1}) are favourable for routine Magic Angle Spinning (MAS) experiments, the acquisition of simple one-dimensional spectra is time consuming, particularly for these materials that contain low loadings of minor surface species (surface densities as low as 0.06 tin species nm^{-2}). Recently we showed that DNP SENS accelerates the acquisition of NMR spectra of surface species by several orders of magnitude compared to standard room temperature experiments.[17] In DNP SENS a polarizing agent, in this case the stable nitroxyl diradical TEKPol (Figure 2),[23] is introduced to the material by incipient wetness impregnation in 1,1,2,2-tetrachlorethane.[24] The sample is frozen at *ca.* 100 K in a low temperature NMR probe within a commercial Bruker 400 MHz/263 GHz (9.4 T) DNP system,[25] and microwaves are applied to saturate the EPR transition of the biradical under MAS. This method enhances the polarization of the ^{1}H nuclei of the solvent and the surface species. The enhanced ^{1}H polarization is then transferred to surface hetero-nuclei (i.e., ^{13}C, [29]Si and [119]Sn) with cross polarization (CP).[17]
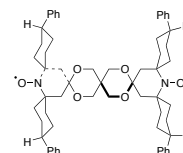
Figure 2. Structure of TEKPol.

To obtain better sensitivity for the inhomogeneously broadened [119]Sn spectra we acquired the DNP SENS spectra with a cross polarization Carr-Purcell Meiboom-Gill pulse sequence (CP-CPMG).[26-29] The [119]Sn CP-CPMG spectra acquired with and without microwave irradiation are shown in Figure 3a and 3b, respectively. DNP enhancement factors, defined as the ratio of the signal intensities of the microwave on spectrum relative to a spectrum recorded without microwaves, of $\varepsilon_{1H} = 116$ and $\varepsilon_{119Sn\ CP} = 56$ were obtained for this material.
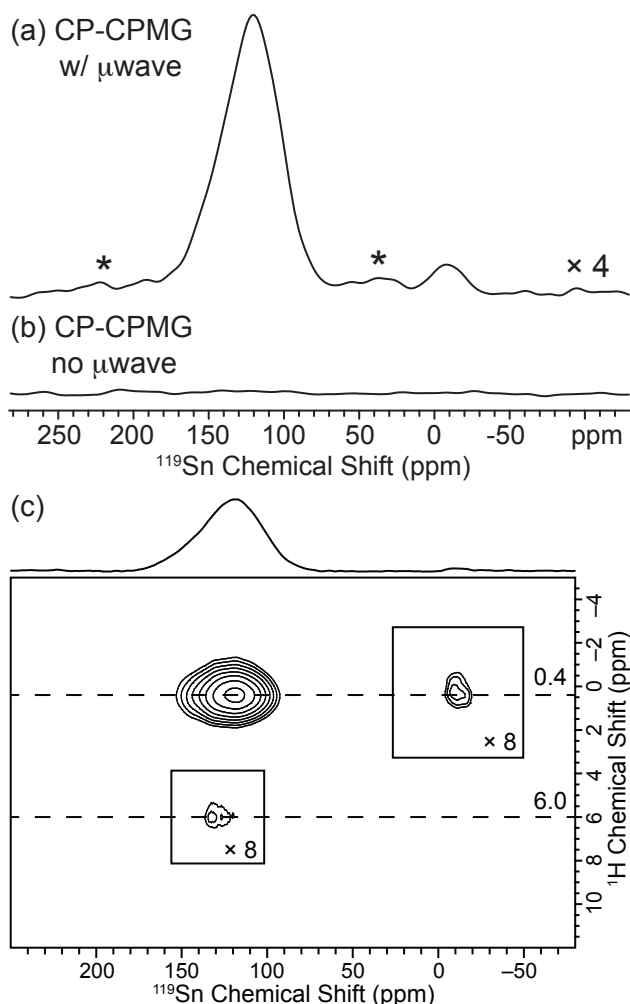

Figure 3. 9.4 T DNP SENS MAS spectra of SnBu₃allyl @ [SiO₂₋₇₀₀] impregnated with 14.1 mM solution of TEKPol in 1,1,2,2-tetrachlorethane. Echo re-constructed [1]H–[119]Sn CP-CPMG spectra (a) with μwave irradiation and (b) without μwave irradiation. 32 and 128 scans were acquired for a and b, respectively. In both cases spectra were acquired with a 4.5 s recycle delay and a 12.5 kHz MAS frequency. Asterisks denote spinning sidebands. (c) [1]H–[119]Sn dipolar HETCOR with a contact time of 0.5 ms. The spectrum was acquired with a 4.0 s recycle delay, 64 scans per increment, 80 individual t_1 increments and a 64 ms t_1 increment (5.7 hours total). During t_1 e-DUMBO-1₂₂ homo-nuclear ^{1}H dipolar decoupling[30] was applied and proton chemical shifts were corrected by applying a scaling factor of 0.57.

The [119]Sn CPMAS spectrum for the [SiO₂₋₇₀₀] material shown in Figure 1a contains two broad peaks centred at 122 and –8 ppm. The major peak centred at 122 ppm is assigned to the *mono*-grafted [(≡SiO)SnBu₃] species, and is consistent with the chemical shifts reported for molecular Bu₃SnOR species.[10] Note that this signal is not symmetric and indicates that there are probably slight variations in the tin environment in [(≡SiO)SnBu₃], consistent with the DFT calculations presented below. The minor resonance centred at –8 ppm is assigned to a *bis*-grafted surface tin species due to the similar [119]Sn chemical shift reported for molecular R₂Sn(OR)₂ compounds in solution.[31, 32] Under DNP SENS conditions we also recorded [29]Si CPMAS spectra, and only signals typical of Q₄-bulk silica overlapping with Si-O-Sn sites[19] were observed (Figure S3). Since DNP SENS is much more sensitive than standard solid state NMR we would expect to see an organosilicon *T*-site under these conditions if it were present. The absence of *T*-sites unambiguously establishes that alkyl transfer does not occur during alkyltin grafting on [SiO₂₋₇₀₀]. The signal enhancement provided by DNP SENS enabled acquisition of a [1]H – [119]Sn HETCOR spectrum in less than 6 hours. The [1]H – [119]Sn HETCOR is shown in Figure 2c, and shows correlations between the two tin resonances and the protons of the butyl group at *ca.* 0.4 ppm. A weak correlation to solvent molecules is also observed for the major tin species. [1]H-^{13}C HETCOR experiments indicate that the protons of the butyl groups possess shifts between 0.3 and 1.0 ppm (Figure S4). The correlations observed in [1]H-[119]Sn and [1]H-^{13}C HETCOR spectra are therefore consistent with alkyl tin species grafted on silica.

DNP SENS also enables natural isotopic abundance [13]C{[119]Sn} REDOR[32] experiments which confirm the spatial proximity of tin to the butyl groups. In a REDOR experiment[33-35] two ^{13}C CP spin echo spectra are acquired. One spectrum is acquired with rotor-synchronized [119]Sn π-pulses applied during the echo delays (dephasing spectrum, *S*), while the other is acquired without any [119]Sn pulses (control spectrum, S_0). The [119]Sn π-pulses re-introduce [119]Sn-^{13}C dipolar couplings and cause reductions in ^{13}C echo intensities (as compared to a control spectrum) for ^{13}C nuclei that are dipolar coupled (proximate) to [119]Sn nuclei. Because of the low isotopic abundance of [119]Sn (N.A. = 8.59 %) the ^{13}C signal in the dephasing spectrum can be reduced at most by a factor of 8.6 % in comparison to the control spectrum. DNP SENS enables acquisition of high signal to noise ratio REDOR ^{13}C spectra, ensuring that reduced signal from [119]Sn dephasing can be discerned from variations in the noise levels of the control and dephasing spectra.

The results of the [13]C{[119]Sn} REDOR[32] experiments are shown in Figure 4. The green circles in Figure 3a correspond to the ratio of the integrated intensities of the dephasing and control spectra (the REDOR fraction, S/S_0) for the whole alkyl region of the spectra (40 ppm to 0 ppm). As the total recoupling time is increased it can be seen that the REDOR fraction approaches 0.91, the value expected for naturally abundant [119]Sn. Predicted REDOR curves[36] are shown for the average one, two, three and four-bond Sn-C inter-atomic distances obtained from quantum chemical calculations of the mono-grafted tri-butyl tin species (*vide infra*). The weighted average of the four simulated curves (solid black line, Figure 2B), with the weightings obtained from a four carbon fit of the ^{13}C REDOR spectra, adequately reproduces the experimental data points. Therefore, the REDOR measurements directly confirm the presence of an alkyl tin surface species.

The [119]Sn DNP SENS spectra of Bu₃Sn(allyl) functionalized [SiO₂₋₈₀₀] and [SiO₂₋₁₀₀₀] materials are nearly identical to the [SiO₂₋₇₀₀] material (Figures S6 and S7). Consistent with the volatile analysis, [SiO₂₋₃₀₀] and [SiO₂₋₅₀₀] materials have [119]Sn DNP SENS spectra that are dominated by the signal at 122 ppm associated with the monografted [(≡SiO)SnBu₃], while only very minor amounts of *bis*-grafted tin was present (Figure S8 and S9). In all cases the DNP SENS ^{13}C CPMAS spectra do not contain resonances

associated with alkyl transfer to the silica surface. Taken together these results indicate that *bis*-grafted species only form on silica dehydroxylated at or above 700 °C.
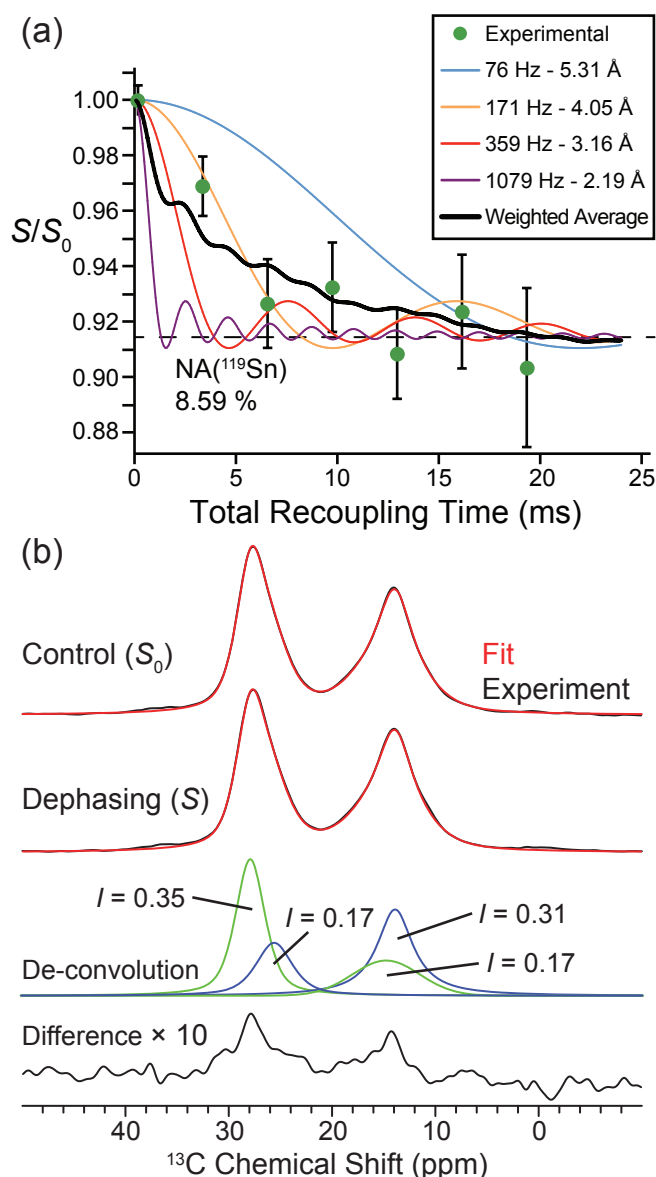

Figure 4. Summary of $^{13}C\{^{119}Sn\}$ REDOR experiments.[32] (a) REDOR signal fraction (S/S_0) as a function of the total recoupling time. Experimental points are indicated as green circles and are taken as the ratio of the integrated intensities of the alkyl region. Analytical REDOR signal fractions are shown for the four different average ^{13}C-^{119}Sn inter-atomic distances obtained from DFT calculations. (b) Typical DNP enhanced REDOR ^{13}C spectra (acquired with a 3.36 ms total recoupling time). The control spectrum (S_0, no ^{119}Sn pulses), the dephasing spectrum (S, with ^{119}Sn pulses), a four site de-convolution of the dephasing spectrum and the difference spectrum ($S_0 - S$) are shown. Experimental spectra are shown in black and four site fits are shown in red for the control and dephasing spectrum.

Identification of the Major and Minor Species from DFT Calculations

We modelled several tin grafted silica species using DFT cluster models of the different silanol sites to determine the energetics of the reactions and the associated ^{119}Sn NMR signatures (chemical shift)

as a function of surface silica site. Note that it is necessary to introduce relativistic effects up to spin orbit coupling to obtain accurate calculated NMR chemical shifts.[37] The results of this study are shown in Figure 5. The formation of the monografted [≡SiOSnBu₃] is exoenergetic (ΔE) by −134 kJ/mol (ΔG = −107 kJ/mol) and the associated calculated ^{119}Sn chemical shift is 110 ppm, a value in agreement with the chemical shift obtained experimentally for the major species (122 ppm). It is noteworthy that the calculated chemical shift of [≡SiOSnBu₃] is very sensitive to minor structural changes and can be as low at 82 ppm (Figure S12) that probably explains the very broad experimental signal resulting from surface species in various local environments.
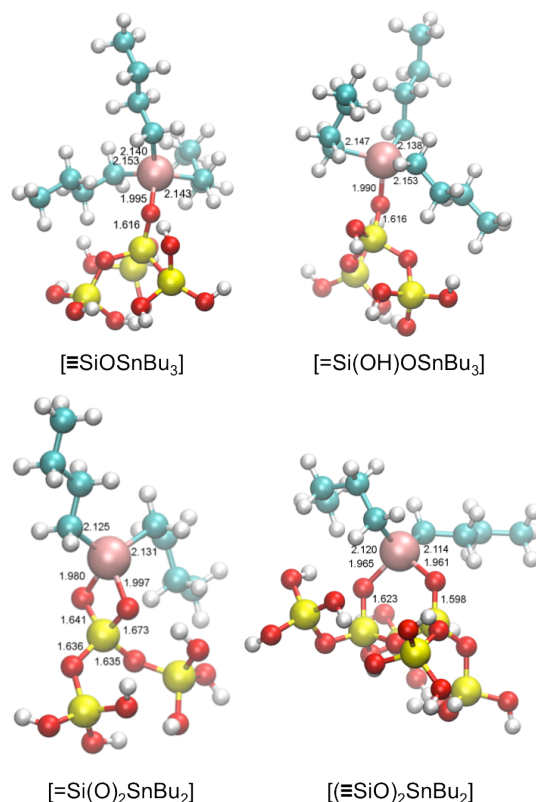

[≡SiOSnBu₃]

[=Si(OH)OSnBu₃]

[=Si(O)₂SnBu₂]

[(≡SiO)₂SnBu₂]

Figure 5. DFT-optimized structures (distances in Å) for the evaluated Sn complexes.

We also optimized two structures that could account for a *bis*-grafted tin species that should correspond to the Sn species at −8 ppm: [=Si(O)₂SnBu₂], and [(≡SiO)₂SnBu₂]. We included [=Si(OH)OSnBu₃] as a likely intermediate in the formation of *bis*-grafted tin species. The formation of [=Si(OH)(OSnBu₃)] is favourable (ΔE = −144 kJ/mol with ΔG = −122 kJ/mol) and the associated ^{119}Sn chemical shift is 110 ppm, and is within the experimentally observed signal and cannot be distinguished from [≡SiOSnBu₃]. The *bis*-grafted [=Si(O)₂SnBu₂] that would form from the direct reaction of a geminal Q_2-dislanol and Bu₃Sn(allyl), is energetically favoured by −95 kJ/mol. While entropically favoured because of the release of butane and propene (ΔG = −126 kJ/mol), the associated surface species display a calculated ^{119}Sn chemical shift of 79 ppm, which is somewhat low to be compatible with the experimental value, and is clearly not associated with the minor signal at −8 ppm. In contrast, [(≡SiO)₂SnBu₂], which formally results from the reaction of allyltributyltin with two Q_3-silanols, has a calculated ^{119}Sn chemical shift of −6 ppm, consistent with that

observed experimentally (−8 ppm). The formation of [(≡SiO)$_2$SnBu$_2$] is more favorable (ΔE = −178 kJ mol^{-1} and ΔG = −207 kJ/mol) than [=Si(O)$_2$SnBu$_2$]. This computational analysis reveals that these three calculated structures are energetically favourable, but that only [(≡SiO)$_2$SnBu$_2$] has a calculated NMR chemical shift that matches the experimental minor signal at −8 ppm.

Discussion

Grafting Bu$_3$Sn(allyl) on silica partially dehydroxylated at temperatures ≥ 700 °C results in the formation of two surface species from analysis of the volatile reaction products and ^{119}Sn DNP SENS. While the major species can clearly be assigned to [(≡SiO)SnBu$_3$] and results from the reaction of Bu$_3$Sn(allyl) with isolated silanols, the minor species associated with the signal at −8 ppm is [(≡SiO)$_2$SnBu$_2$] according to DFT calculations. While such species should be formally generated from the reaction of two Q_3-vicinal silanols with the alkyltin reagent, silica dehydroxylated at or above 700 °C does not contain these requisite Q_3-vicinal silanols. In addition, if vicinal silanols were responsible for the formation of such species, one would expect a larger amount of such species formed on [SiO$_{2-500}$] and [SiO$_{2-300}$]. This is clearly not the case, and [(≡SiO)$_2$SnBu$_2$] must form from an alternative pathway.

In view of the preferred formation of the *bis*-grafted tin species [(≡SiO)$_2$SnBu$_2$] on [SiO$_{2-700}$], [SiO$_{2-800}$], and [SiO$_{2-1000}$] we propose that such species originate from the Q_2-geminal silanols. Since these silicas also contain strained siloxane bridges on the surface,[38] we propose that allyltributylstannane reacts first with the Q_2-geminal silanols to form mono-grafted [=Si(OH)OSnBu$_3$] and propene. The remaining silanol can then react with an adjacent strained siloxane bridge, probably activated by the presence of the adjacent tin Lewis acid site, that would result in the unmasking of an adjacent Q_3-silanol (Scheme 2). This silanol would then react with the Bu-Sn fragment to liberate butane and form [(≡SiO)$_2$SnBu$_2$]. Such surface rearrangements involving the opening of siloxane bridges and the movement of silanols have been proposed when Lewis acidic metals come in contact with dehydroxylated silica.[39, 40] We should note again that this reactivity is somewhat unusual in that most siloxane bridge openings follow alkyl transfter to the surface that forms alkyl-silicon surface species.[20, 22, 41, 42]
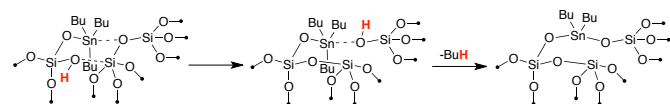
Scheme 2. Proposed formation of [(≡SiO)$_2$SnBu$_2$] from [=Si(OH)OSnBu$_3$] and strained siloxane bridges.

Conclusions

We described the reaction of [SiO$_{2-700}$] and allyltributylstannane. While the isolated silanols on [SiO$_{2-700}$] react as expected to form mono-grafted [≡SiOSnBu$_3$], the geminal Q_2-silanols react in an unexpected manner. While the formation of [=Si(O)$_2$SnBu$_2$] or [=Si(OH)(O-SnBu$_3$)] species is expected from reaction with =Si(OH)$_2$, DNP SENS characterization in combination with DFT calculations clearly indicate the formation of [(≡SiO)$_2$SnBu$_2$]. The formation of [(≡SiO)$_2$SnBu$_2$] only occurs for silica dehydroxylated at or above 700 °C that contains a low density of surface silanols and strained siloxane bridges. Evidently the driving force for this chemistry is relief of the strained siloxane bridges, revealing the complexity and flexibility of the silica support. Finally we should note that this study has been greatly helped by

^{119}Sn DNP SENS because it allows the detection of minor surface species, such as [(≡SiO)$_2$SnBu$_2$], present on the surface in low abundance (<0.1 .nm^{-2}) in a reasonable measurement time. We are currently exploring the detailed surface chemistry of hydroxylated surfaces with DNP SENS.

Notes and references

^{a} Department of Chemistry and Applied Biosciences, Vladimir Prelog Weg 2 ETH Zürich, CH-8093 Zürich, Switzerland.
^{b} Centre de RMN à Très Hauts Champs, Université de Lyon (CNRS/ENS Lyon/UCB Lyon 1), 69100 Villeurbanne, France.
^{c} Aix-Marseille Université, CNRS, ICR UMR 7273, Faculté de Saint Jérôme case 521, 13397 Marseille Cedex 20 (France)
† Footnotes should appear here. These might include comments relevant to but not central to the matter under discussion, limited experimental and spectral data, and crystallographic data.
Electronic Supplementary Information (ESI) available: SENS NMR spectra of all materials and computational details See DOI: 10.1039/b000000x/

1. C. Copéret, M. Chabanas, R. Petroff Saint-Arroman and J.-M. Basset, *Angewandte Chemie International Edition*, 2003, **42**, 156-181.
2. J. M. Thomas, R. Raja and D. W. Lewis, *Angewandte Chemie International Edition*, 2005, **44**, 6456-6482.
3. S. L. Wegener, T. J. Marks and P. C. Stair, *Accounts of Chemical Research*, 2011, **45**, 206-214.
4. J. M. Basset, J. P. Candy and C. Copéret, in *Comprehensive Organometallic Chemistry III*, eds. H. C. Editors-in-Chief:¬†¬† Robert and D. M. P. Mingos, Elsevier, Oxford, 2007, pp. 499-553.
5. T. J. Marks, *Accounts of Chemical Research*, 1992, **25**, 57-65.
6. L. T. Zhuravlev, *Colloids and Surfaces A: Physicochemical and Engineering Aspects*, 2000, **173**, 1-38.
7. A. Rimola, D. Costa, M. Sodupe, J.-F. o. Lambert and P. Ugliengo, *Chemical Reviews*, 2013, **113**, 4216-4313.
8. P. Hoffmann and E. Knözinger, *Surface Science*, 1987, **188**, 181-198.
9. J. van der Meer, I. Bardez-Giboire, C. Mercier, B. Revel, A. Davidson and R. Denoyel, *The Journal of Physical Chemistry C*, 2010, **114**, 3507-3515.
10. C. Nedez, A. Theolier, F. Lefebvre, A. Choplin, J. M. Basset and J. F. Joly, *Journal of the American Chemical Society*, 1993, **115**, 722-729.
11. C. Nedez, A. Choplin, F. Lefebvre, J. M. Basset and E. Benazzi, *Inorganic Chemistry*, 1994, **33**, 1099-1102.
12. C. Nedez, F. Lefebvre, A. Choplin, J. M. Basset and E. Benazzi, *Journal of the American Chemical Society*, 1994, **116**, 3039-3046.
13. X. X. Wang, A. de Mallmann, F. Bayard, F. Lefebvre and J. M. Basset, *Microporous Mesoporous Mater.*, 2003, **63**, 147-161.
14. J.-W. Park, Y. J. Park and C.-H. Jun, *Chemical Communications*, 2011, **47**, 4860-4871.
15. A. Lesage, M. Lelli, D. Gajan, M. A. Caporini, V. Vitzthum, P. Miéville, J. Alauzun, A. Roussey, C. Thieuleux, A. Mehdi, G.

Bodenhausen, C. Coperet and L. Emsley, *Journal of the American Chemical Society*, 2010, **132**, 15459-15461.

16. M. Lelli, D. Gajan, A. Lesage, M. A. Caporini, V. Vitzthum, P. Miéville, F. Héroguel, F. Rascon, A. Roussey, C. Thieuleux, M. Boualleg, L. Veyre, G. Bodenhausen, C. Coperet and L. Emsley, *Journal of the American Chemical Society*, 2011, **133**, 2104-2107.

17. A. J. Rossini, A. Zagdoun, M. Lelli, A. Lesage, C. Cop√©ret and L. Emsley, *Accounts of Chemical Research*, 2013, **46**, 1942-1951.

18. L. Protesescu, A. J. Rossini, D. Kriegner, M. Valla, A. de Kergommeaux, M. Walter, K. V. Kravchyk, M. Nachtegaal, J. Stangl, B. Malaman, P. Reiss, A. Lesage, L. Emsley, C. Copéret and M. V. Kovalenko, *ACS Nano*, 2014.

19. K. Chaudhari, T. K. Das, P. R. Rajmohanan, K. Lazar, S. Sivasanker and A. J. Chandwadkar, *J. Catal.*, 1999, **183**, 281-291.

20. H. Ahn and T. J. Marks, *Journal of the American Chemical Society*, 2002, **124**, 7103-7110.

21. E. Le Roux, M. Chabanas, A. Baudouin, A. de Mallmann, C. Copéret, E. A. Quadrelli, J. Thivolle-Cazat, J.-M. Basset, W. Lukens, A. Lesage, L. Emsley and G. J. Sunley, *Journal of the American Chemical Society*, 2004, **126**, 13391-13399.

22. F. Rataboul, A. Baudouin, C. Thieuleux, L. Veyre, C. Copéret, J. Thivolle-Cazat, J.-M. Basset, A. Lesage and L. Emsley, *Journal of the American Chemical Society*, 2004, **126**, 12541-12550.

23. A. Zagdoun, G. Casano, O. Ouari, M. Schwarzw√§lder, A. J. Rossini, F. Aussenac, M. Yulikov, G. Jeschke, C. Cop√©ret, A. Lesage, P. Tordo and L. Emsley, *Journal of the American Chemical Society*, 2013, **135**, 12790-12797.

24. A. Zagdoun, A. J. Rossini, D. Gajan, A. Bourdolle, O. Ouari, M. Rosay, W. E. Maas, P. Tordo, M. Lelli, L. Emsley, A. Lesage and C. Coperet, *Chemical Communications*, 2012, **48**, 654-656.

25. M. Rosay, L. Tometich, S. Pawsey, R. Bader, R. Schauwecker, M. Blank, P. M. Borchard, S. R. Cauffman, K. L. Felch, R. T. Weber, R. J. Temkin, R. G. Griffin and W. E. Maas, *Physical Chemistry Chemical Physics*, 2010, **12**, 5850-5860.

26. I. Hung, A. J. Rossini and R. W. Schurko, *J. Phys. Chem. A*, 2004, **108**, 7112-7120.

27. R. Siegel, T. T. Nakashima and R. E. Wasylishen, *The Journal of Physical Chemistry B*, 2004, **108**, 2218-2226.

28. J. Trebosc, J. W. Wiench, S. Huh, V. S. Y. Lin and M. Pruski, *Journal of the American Chemical Society*, 2005, **127**, 7587-7593.

29. A. J. Rossini, A. Zagdoun, M. Lelli, D. Gajan, F. Rascon, M. Rosay, W. E. Maas, C. Coperet, A. Lesage and L. Emsley, *Chemical Science*, 2012, **3**, 108-115.

30. B. Elena, G. l. de Paepe and L. Emsley, *Chem. Phys. Lett.*, 2004, **398**, 532-538.

31. C. Nedez, V. Dufaud, F. Lefebvre, J. M. Basset and B. Fenet, *C. R. Chim.*, 2004, **7**, 785-796.

32. P. J. Smith, R. F. M. White and L. Smith, *Journal of Organometallic Chemistry*, 1972, **40**, 341-353.

33. T. Gullion, *Concepts in Magnetic Resonance*, 1998, **10**, 277-289.

34. Y. Pan, T. Gullion and J. Schaefer, *Journal of Magnetic Resonance (1969)*, 1990, **90**, 330-340.

35. T. Gullion and J. Schaefer, *Journal of Magnetic Resonance (1969)*, 1989, **81**, 196-200.

36. K. T. Mueller, *Journal of Magnetic Resonance, Series A*, 1995, **113**, 81-93.

37. A. Bagno, G. Casella and G. Saielli, *J. Chem. Theory Comput.*, 2005, **2**, 37-46.

38. J. Li, J. A. DiVerdi and G. E. Maciel, *Journal of the American Chemical Society*, 2006, **128**, 17093-17101.

39. P. Mania, S. Conrad, R. Verel, C. Hammond and I. Hermans, *Dalton Transactions*, 2013, **42**, 12725-12732.

40. P. Mania, R. Verel, F. Jenny, C. Hammond and I. Hermans, *Chemistry – A European Journal*, 2013, **19**, 9849-9858.

41. S. L. Scott and J.-M. Basset, *Journal of the American Chemical Society*, 1994, **116**, 12069-12070.

42. B. A. Morrow and I. A. Cody, *J. Phys. Chem.*, 1976, **80**, 1995-1998.